BJP British Journal of Pharmacology

DOI:10.1111/j.1476-5381.2012.01899.x
www.brjpharmacol.org

RESEARCH PAPER

Uncoupling of sarcoplasmic reticulum Ca^{2+}-ATPase by *N*-arachidonoyl dopamine. Members of the endocannabinoid family as thermogenic drugs

YA Mahmmoud[1] and M Gaster[2]

[1]*Department of Biomedicine, University of Aarhus, Aarhus C, Denmark, and* [2]*Laboratory of Molecular Physiology, Department of Pathology and Endocrinology, University Hospital of Odense, Odense, Denmark*

Correspondence
YA Mahmmoud, Department of Biomedicine, University of Aarhus, DK-8000 Aarhus C, Denmark. E-mail: yam@biophys.au.dk

Keywords
SERCA; *N*-arachidonoyl dopamine; uncoupling; thermogenesis; ATP depletion; Ca^{2+}-ATPase; oligomycin

Received
18 October 2011
Revised
31 January 2012
Accepted
7 February 2012

BACKGROUND AND PURPOSE

The sarcoplasmic reticulum Ca^{2+}-ATPase (SERCA) plays a role in thermogenesis. The exogenous compound capsaicin increased SERCA-mediated ATP hydrolysis not coupled to Ca^{2+} transport. Here, we have sought to identify endogenous compounds that may function as SERCA uncoupling agents.

EXPERIMENTAL APPROACH

Using isolated SR vesicles from rabbits, we have screened for endogenous compounds that uncouple SERCA. We have also studied their ability to deplete cytoplasmic ATP from human skeletal muscle cells in culture.

KEY RESULTS

Studies on SR vesicles showed that the endogenous lipid metabolite *N*-arachidonoyl dopamine (NADA) was a potent stimulator of SERCA uncoupling. NADA stabilized an E_1-like pump conformation that had a lower dephosphorylation rate, low affinity for Ca^{2+} at the luminal sites and a specific proteinase K cleavage pattern involving protection of the C-terminal p83C fragment from further cleavage. Moreover, we found a significantly decreased cytoplasmic ATP levels following treatment of skeletal muscle cells with 100 nM NADA. This effect was dependent on the presence of glucose and abolished by pretreatment with the specific SERCA inhibitor thapsigargin, regardless of the presence of glucose.

CONCLUSIONS AND IMPLICATIONS

NADA is an endogenous molecule that may function as SERCA uncoupling agent *in vivo*. Members of the endocannabinoid family exert concerted actions on several Ca^{2+}-handling proteins. Uncoupling of SERCA by exogenous compounds could be a novel post-mitochondrial strategy for reduction of cellular ATP levels. In addition, signalling networks leading to SERCA uncoupling can be explored to study the importance of this ion pump in pathophysiological conditions related to metabolism.

Abbreviations

DMEM, Dulbecco's modified Eagle's medium; ECM, extracellular matrix; FCS, fetal calf serum; NADA, *N*-arachidonoyl dopamine; PrtK, proteinase K; SERCA, Sarco(endo)plasmic reticulum Ca^{2+}-ATPase; Na^+/K^+-ATPase, sodium- and potassium- activated adenosine triphosphatase; TRPV, transient receptor potential vanilloid; TCA, trichloroacetic acid

Introduction

Many cellular events are associated with dynamic changes in cytoplasmic calcium concentration. In the working muscle, sarcoplasmic reticulum (SR) Ca^{2+}-ATPase (EC 3.6.3.8, SERCA1) rapidly clears cytoplasmic Ca^{2+} to ensure prompt muscle relaxation. SERCA uses energy from ATP hydrolysis to build up a Ca^{2+} gradient across the SR membrane, which can reach up to four orders of magnitude. Early biochemical and molecular biology studies (Andersen, 1995; MacLennan *et al.*, 1997; Kühlbrandt, 2004) as well as structural studies over the last 11 years (Toyoshima *et al.*, 2000; 2004; Olesen *et al.*, 2004; 2007) have made SERCA the best characterized P-type pump.

In rabbit skeletal muscle, cold acclimatization studies have unambiguously identified SERCA as a primary element in oxygen consumption and non-shivering thermogenesis (Arruda *et al.*, 2008). In contrast to the wealth of information known about its structure and mechanism, the regulation of thermogenesis by SERCA is poorly understood. Indeed, an increase in cytoplasmic Ca^{2+} concentration through passive routes is usually considered a prerequisite for stimulation of SERCA and dissipation of heat as a by-product. For consistency, excessive heat generation by SERCA in malignant hyperthermia is a consequence of anomalous Ca^{2+} influxes through an abnormal ryanodine receptor 1 (McCarthy *et al.*, 2000). Hence, Ca^{2+} mobilization is considered an essential mediator of thermogenesis.

Uncoupling between Ca^{2+} transport to the SR lumen and ATP hydrolysis has been studied intensively *in vitro* (Mitidieri and de Meis, 1999; Barata and de Meis, 2002; de Meis *et al.*, 2005). The mechanistic basis for uncoupling involves either a SERCA-independent increase in passive Ca^{2+} permeation across the SR membrane (such as in malignant hyperthermia) or an increase in passive permeation through SERCA, the latter presumably leading to ATP regeneration (cycle reversal) and not associated with thermogenesis. An alternative mode of SERCA uncoupling in the absence of passive Ca^{2+} leak occurs in SERCA reconstituted into liposomes and it was postulated that hydrolytic cleavage can proceed without Ca^{2+} translocation to the SR lumen (Yu and Inesi, 1995). Under these conditions, the energy from ATP hydrolysis dissipates as heat.

We have previously shown that capsaicin, a plant-derived vanilloid, increases ATP hydrolysis by SERCA without effects on Ca^{2+} accumulation. We have proposed that increased thermogenesis that follows capsaicin may occur through a direct effect on SERCA (Mahmmoud, 2008). Now the question arises how uncoupling of SERCA, if any, can be ligand-controlled in living cells and, if so, does SERCA uncoupling occur in muscle tissue by yet unrecognized effectors? We anticipated the existence of endogenous ligands that may behave similarly to capsaicin, and we have consequently investigated several compounds for their ability to stimulate ATP hydrolysis by SERCA. The screening was based on the fact that capsaicin is functionally homologous to several endogenous lipid metabolites of the multifunctional endocannabinoid family of molecules, which are effectors of the cannabinoid receptors in the CNS (Scotter *et al.*, 2010), and vanilloid receptors in sensory neurons (Szallasi and Blumberg, 1999). Interestingly, several members of the endocannabinoid family have been detected in human plasma (Balverg *et al.*, 2009). *N*-arachidonoyl dopamine (NADA) has also been described in rat brain (Huang *et al.*, 2002). Here, we present NADA as a potential stimulator of ATP hydrolysis by SERCA and we show that NADA uncoupled SERCA by a mechanism distinct from that of capsaicin. In addition, NADA significantly decreased ATP levels in cultures of human skeletal muscle cells in a manner that was dependent on the presence of functional SERCA. Hence, SERCA-uncoupling compounds may be considered a tool in studies involving transient or sustained depletion of cellular ATP, downstream of the conventional ATP depletion strategy that involves the use of non-specific macrolide inhibitors of ATP synthesis in mitochondria.

Methods

Enzyme preparation and hydrolytic activity

All animal care and experimental procedures complied with the guidelines described by the Danish center for animal welfare. The results of all studies involving animals are reported in accordance with the ARRIVE guidelines for reporting experiments involving animals (McGrath *et al.*, 2010). Rabbits (males or females of the Danish farm strain, aged about 2 years; total number, 4) were killed by an authorized person using a captive bolt device. SR vesicles were prepared from rabbit fast twitch skeletal muscle (quadriceps femoris). The preparation method involves mincing and blending the tissue (~400 g) in a buffer (1200 mL) containing 100 mM KCl, 2 mM EDTA, 2.5 mM KH_2PO_4, and 2.5 mM K_2HPO_4, followed by differential centrifugation, as described previously (de Meis and Hasselbach, 1971). The purified SR vesicles used in this study was a generous gift of Professor Jesper V. Møller. Purified SR proteins were treated with DMSO or the compound of interest, followed by ATPase measurements. Ca^{2+}-dependent SERCA-mediated ATP hydrolysis was measured in a reaction mixture containing 20 mM 3-(n-morpholino)propanesulfonic acid (MOPS), pH 7, 80 mM KCl, 20 mM NaCl, 5 mM $MgCl_2$, 0.5 mM EGTA, 2–4% DMSO (including drugs). Free Ca^{2+} concentrations are shown in separate figure legends. In all experiments described in this study, the final concentration of DMSO did not exceed 4%.

Pig kidney Na^+/K^+-ATPase was prepared as described previously (Klodos *et al.*, 2002) from tissue obtained from a licensed abbatoir. Ouabain-specific Na,K-ATPase was measured in the presence of 20 mM histidine buffer, pH 7, 100 mM NaCl, 20 mM KCl, 3 mM $MgCl_2$, 3 mM ATP, 2 µg pig renal medulla membranes. Phosphate liberated from ATP hydrolysis was measured using a calorimetric method, as described previously (Mahmmoud and Christensen, 2011).

Phosphorylation/dephosphorylation reactions

Phosphorylation from inorganic phosphate (P_i) was performed in a buffer (500 µL) containing 25 mM MOPS, pH 6.5, 1 mM EGTA, 50 µg SR protein, 10 mM $MgCl_2$, the phosphate concentrations indicated in Fig. 3A and either DMSO control or 20 µM NADA. The reaction was terminated with the addition of 1.5 mL stopping solution containing 24% TCA and 6 mM P_i (sodium salt). After washing and

collection, the radioactivity associated with the protein was determined by scintillation counting. For dephosphorylation, the phopshorylated enzyme was diluted 10 times in dephosphorylation buffer and the reaction was stopped with acid after different time intervals, before washing and collection.

Proteolytic cleavage

SDS-PAGE was performed as described previously (Mahmmoud, 2008). Phosphorylation was performed in 44 mM MOPS buffer, 50 mM KCl, 2 mM EGTA, 2 mM $MgCl_2$, 0.72 mM ATP and 50 μg SR protein. The free Ca^{2+} concentration was adjusted to 40–45 μM. Following incubation at room temperature for 5 min, 1 μg proteinase K (PrtK) was added and the mixture incubated for 40 min at 24°C. For phosphorylation from P_i, the reaction was the same as mentioned earlier except that 5 mM Na_2HPO_4 replaced ATP, Ca^{2+} was omitted, and the phosphorylation reaction proceeded for 15 min before the addition of PrtK. The reaction stopped with SDS sample buffer containing 1% TCA to ensure complete deactivation of PrtK. Samples were separated by electrophoresis on 8% tricine-based gels and stained with Coomassie blue. Scanning and intensity determination of the autoradiograms was performed using ImageQuant TL image analysis software (Amersham Biosciences, Buckinghamshire, UK).

Human study subjects

Muscle biopsies (200–300 mg) were obtained from the vastus lateralis muscle by needle biopsy under local anaesthesia from five healthy lean men (age between 44–53 years). All subjects gave written informed consent, and the local ethics committee of Funen and Vejle County approved the study.

Cell culture

Cell cultures were established as previously described (Gaster *et al.*, 2001a,b). In brief, muscle tissue was minced, washed, and dissociated for 60 min by three treatments with 0.05% trypsin-EDTA. The harvested cells were pooled and fetal calf serum (FCS) was added to stop trypsination. The cells obtained were seeded at a density of 4000 cells·cm^{-2} in extracellular matrix (ECM) gel-coated dishes after 30 min of preplating. Cell cultures were established in DMEM medium supplemented with 10% FCS, 50 U·mL^{-1} penicillin, 50 μg·mL^{-1} streptomycin and 1.25 μg·mL^{-1} amphotericin B. After 24 h, cell debris and non-adherent cells were removed by change of growth medium to DMEM supplemented with 2% FCS, 2% Ultroser G, 50 U·mL^{-1} penicillin, 50 μg·mL^{-1} streptomycin and 1.25 μg·mL^{-1} amphotericin B. Cells were subcultured twice before final seeding (4–6 weeks). At 75% confluence, the growth medium was replaced by basal medium (DMEM supplemented with 2% FCS, 50 U·mL^{-1} penicillin, 50 μg·mL^{-1} streptomycin, 1.25 μg·mL^{-1} amphotericin B and 25 pM insulin) in order to induce differentiation. The cells were cultured in humidified 5% CO_2 atmosphere at 37°C, and medium was changed every 2–3 days.

Treatment with drugs and ATP determination

Human myotubes were allowed to differentiate under physiological conditions of insulin (25 pM) and glucose (5.5 mM). All myotube cultures were used for analysis 4 days after onset of differentiation. Myotubes were exposed to 0.1 μM NADA supplemented with or without 400 nM thapsigargin and with or without 5 mM glucose followed by determination of myocellular ATP content after different time periods (Gaster, 2007). ATP was determined with the ATP monitoring reagent (ATPlite from PerkinElmer, Turku, Finland) in 96-well plates and determined by luminescence on a Microbeta counter (PerkinElmer).

Data analysis

Data in Figures 1, 2A and 3A were fitted using a hyperbolic function; $y = \frac{y_{max} \cdot x}{K_d + x}$, where K_d is the equilibrium-binding constant. Data in Figure 3B were fitted using the Hill equation; $y = y_0 + \frac{y_{max} - y_0}{1 + 10^{Log(K_i - x)n_H}}$, where y_0 and y_{max} are baseline and maximum activity and x is the concentration of inhibitor. K_i is the inhibitor concentration that gives 50% inhibition and n_H is the Hill coefficient. Data in Figure 4 were fitted using a single exponential decay function; $y = (y_0 - plateau) \cdot e^{-Kt} + plateau$, K is the rate constant of phosphoenzyme decay. Experiments were repeated at least five times, each in duplicate. Results shown are means ± SEM of five independent measurements. ATP measurements were performed on several cell cultures and were repeated at least 10 times. Differences between means were assessed with the unpaired *t*-test. Statistical analysis was performed by one- or two-way ANOVA, followed by Bonferroni's test of multi comparisons. *P*-values are indicated in the legends to the figures, when appropriate. *P*-values less than 0.05 were considered as significant. For results presented in Figure 6, additional unpaired *t*-test was performed to compare a set of two groups. All procedures were taken from Graph Pad Prism (GraphPad Software, Inc., San Diego, CA, USA). The nomenclature for Ca^{2+}-ATPase follows Alexander *et al.*, (2011).

Materials

Dulbecco's modified Eagle's medium (DMEM), FCS, penicillin-streptomycin-amphotericin B, and trypsin-EDTA were obtained from Invitrogen (Scotland, UK). Ultroser G was purchased from Pall Biosepra (Cergy-Saint-Christophe, France). Protein assay kit was purchased from Bio-Rad (Hercules, CA, USA). ECM gel was purchased from Sigma (St Louis, MO, USA). Bovine serum albumin was from VWR. N-oleoyl dopamine and N-palmitoyl dopamine were purchased from Cayman Chemical Company (Ann Arbor, MI, USA). NADA was purchased from Sigma as well as from Cayman. Capsaicin, thapsigargin, resiniferatoxin (RTX), SB 36679 and capsazepine were all from Sigma.

Results

NADA increases ATP hydrolysis by SERCA in tight SR vesicles in the absence of fluoride, but not in its presence

Treatment of SR vesicles with increasing concentrations of NADA resulted in a robust increase in SERCA-mediated ATP hydrolysis, compared with untreated control (Figure 1A). N-oleoyl dopamine and N-palmitoyl dopamine, which are

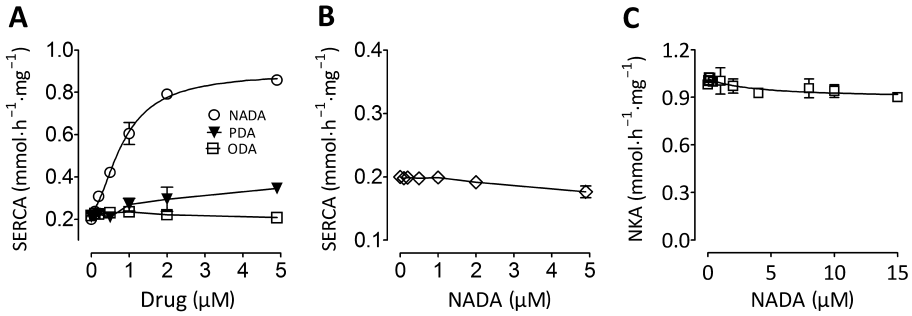

Figure 1

(A) NADA stimulates ATP hydrolysis by SERCA. Ca^{2+}-dependent SERCA-mediated ATP hydrolysis was measured in the presence of the indicated concentrations of NADA, *N*-palmitoyl dopamine (PDA), or *N*-oleoyl dopamine (ODA). For NADA, a hyperbolic equation was fitted to the data points, producing a K_d value of 0.36 ± 0.12 μM. (B) Effects of NADA on SERCA activity was measured as in A, but in the presence of 20 mM NaF. The free Ca^{2+} concentration was calculated as 0.5 μM. (C) Effect of NADA on pig kidney Na,K-ATPase activity (NKA), in the presence of the indicated NADA concentrations.

structurally related to NADA but are shorter (C18 and C16, respectively) and lack hydrocarbon chain polyunsaturation, were also tested for their ability to stimulate ATP hydrolysis by SERCA. At a concentration of 5 μM, N-palmitoyl dopamine had little effect compared with that of NADA, whereas N-oleoyl dopamine did not cause any detectable change in SERCA activity, demonstrating the specificity of NADA as a stimulator of ATP hydrolysis by SERCA.

The energy from SERCA-mediated ATP hydrolysis can either be used to pump Ca^{2+} in the SR lumen (coupled transport), or be dissipated as heat (uncoupled transport). The probability of uncoupling increases as Ca^{2+} accumulates in the SR lumen. It has been shown that uncoupled transport can be dissected from coupled transport by treatment with fluoride, which has been shown to selectively inhibit uncoupled transport but increase the stoichiometric efficiency of Ca^{2+} transport across the SR lumen (Reis *et al.*, 2001). In other words, only the fraction of pumps involved in active transport of Ca^{2+} are active in the presence of fluoride, and pumps sustaining ATP hydrolysis not coupled to transport are inhibited (Reis *et al.*, 2001). NADA did not stimulate SERCA activity in the presence of fluoride, indicating that the NADA did not affect coupled ATP hydrolysis, at least at concentrations below 2 μM. This indicates that the drug stimulates uncoupled ATP hydrolysis (Figure 1B). NADA has no appreciable effect on ATP hydrolysis by the closely related Na^+/K^+-ATPase (Figure 1C), measured at optimum substrate concentrations (see. Mahmmoud and Christensen, 2011). As was the case with capsaicin, NADA did not increase the permeability of liposomes subjected to an electrochemical gradient for Na^+ measured using oxonol IV fluorescence, indicating that NADA *per se* has no effect on membrane permeability in the absence of SERCA (data not shown).

The effect of Ca^{2+} and Ca^{2+} gradient on the interaction of NADA with SERCA

An increase in the cytoplasmic Ca^{2+} concentration is the trigger for activation of the pumping activity of SERCA under physiological conditions. We therefore studied the *in vitro* relationship between extravesicular (cytoplasmic) Ca^{2+} concentration and the equilibrium binding constant for NADA. The extra-vesicular Ca^{2+} concentration strongly affected the equilibrium binding constant for NADA (Figure 2A). Thus, an 80-fold decrease in the extra-vesicular Ca^{2+} concentration (from 40 to 0.5 μM) resulted in ~54-fold decrease in the K_d of NADA (from 17.8 ± 1.6 μM to 0.33 ± 0.09 μM).

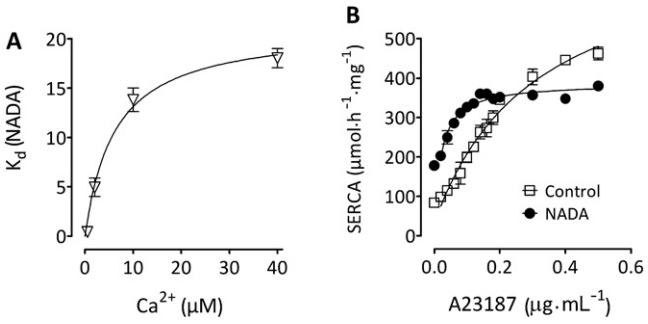

Figure 2

Extravesicular Ca^{2+} and Ca^{2+} gradient across SR membranes are important determinants of NADA activation. (A) Stimulation of SERCA activity by increasing concentrations of NADA was measured, in the presence of the indicated fixed free Ca^{2+} concentrations. The K_d values for the different activation curves were determined by fitting the Hill function to the data, which were then plotted against [Ca^{2+}], as shown. (B) The effect of A23187 on stimulation of ATP hydrolysis by NADA. SERCA activity was measured as in panel A, but in the presence of 12 μM free Ca^{2+}, and with or without 5 μM NADA.

Under conditions of an existing Ca^{2+} gradient across the SR membrane, Ca^{2+} transport to the SR lumen (associated with the $E_1P \rightarrow E_2P$ transition) becomes rate-limiting and the stoichiometric efficiency of SERCA decreases. We have studied how dissipation of the Ca^{2+} gradient using a Ca^{2+} ionophore would affect the stimulation of SERCA by NADA. Results in Figure 2B point to a fundamental difference between NADA and capsaicin (Mahmmoud, 2008); although NADA stimulated ATP hydrolysis by SERCA in the presence of a Ca^{2+} gradient, i.e., at concentrations of A23187 < 0.2 μg·mL^{-1}, no stimulation was observed in the absence of

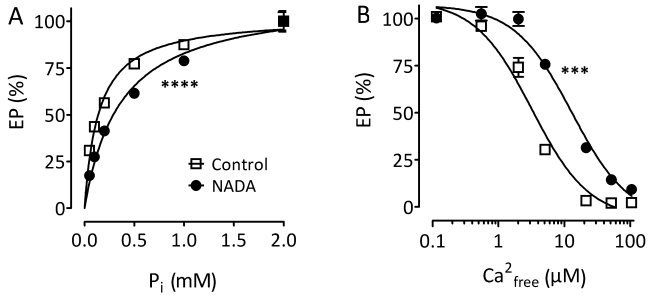

Figure 3

NADA reduces interaction of Ca^{2+} with the luminal sites. (A) Phosphorylation from P_i was measured, in the presence of either DMSO control or 20 μM NADA. A hyperbolic function was used to analyse the data. ****$P < 0.0001$, significantly different from DMSO control; two-way ANOVA. (B) Phosphorylation from P_i was measured as in A. After incubation for 10 min, 1 μg·mL^{-1} A23187 plus the indicated Ca^{2+} concentrations were added and the mixtures incubated for further 5 min before reaction termination and further processing. ***$P < 0.001$, significantly different from DMSO controls; two-way ANOVA.

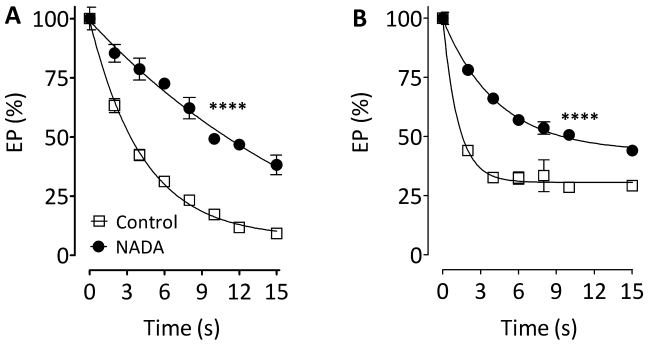

Figure 4

Dephosphorylation of SERCA phosphorylated from ATP. (A) Phosphorylation was performed as described in Methods. The phosphoenzyme reaction mixture (500 μL) was quenched with dilution buffer (1.5 mL of 25 mM MOPS containing 21 mM EGTA/Tris) allowing for rapid Ca^{2+} chelation and bringing the free Ca^{2+} concentration to the pM range. This was followed by acid quenching after the indicated time intervals. Data were analysed by a single exponential decay function. ****$P < 0.0001$, significantly different from DMSO controls; two-way ANOVA. (B) Phosphorylation was performed as in A but the dilution buffer yielded a final concentration of 1 mM ADP. ****$P < 0.0001$, significantly different from DMSO controls; two-way ANOVA.

the gradient, at concentrations of A23187 > 0.2 μg·mL^{-1}, implying that uncoupled ATP hydrolysis was not stimulated in the absence of a Ca^{2+} gradient across the membrane.

NADA shifts the conformational equilibrium of SERCA towards the E_1 form

The dependence of E_2P formation on P_i was measured in the absence and in the presence of NADA (Figure 3A), showing that NADA increased the K_d for phosphorylation from P_i by more than twofold. The K_d for stimulation of EP formation was 142 ± 10 μM for the control and 364 ± 29 μM for the NADA-treated enzyme respectively. This indicates that NADA increases the steady state concentration of the E_1 form, as the phosphorylation reaction was performed in the absence of Ca^{2+} and at the same pH for the control and the NADA-treated enzyme, that is under conditions of identical concentration of ions (see later).

The inhibition by luminal Ca^{2+} of phosphoenzyme formed from P_i was also investigated to further specify the conformational preference of the NADA stabilized form. Thus, SR vesicles were incubated under conditions favouring the formation of E_2P. The intracellular ion binding site is locked in the phosphorylated enzyme and low-affinity Ca^{2+} sites are open at the luminal side (Sørensen *et al.*, 2004). Hence, Ca^{2+} ionophore is added together with increasing Ca^{2+} concentrations to measure the dephosphorylation induced by luminal Ca^{2+}. As seen in Figure 3B, Ca^{2+} inhibition of E_2P formation required significantly higher Ca^{2+} concentrations in the presence of NADA than in its absence. Thus, the K_i values for the control and the NADA-treated enzyme were 2.8 ± 1.0 μM and 12.3 ± 1.1 μM respectively. Hence, NADA decreases Ca^{2+} interaction with the luminal site(s) by directly affecting the luminal sites or shifting the conformation of SERCA towards the E_1 conformation (at which the luminal sites are closed).

NADA decreases the dephosphorylation rate

The effect of NADA on the dephosphorylation of enzyme phosphorylated from ATP was investigated. Interestingly, NADA sustains the opposite effect of capsaicin, namely, the dephosphorylation rate of the NADA-treated enzyme is less than untreated controls. Thus, the addition of excess EGTA (to remove extra-vesicular Ca^{2+}) to a phosphoenzyme mixture under steady state conditions, resulted in rapid dephosphorylation of SERCA (k ~ 0.24 s^{-1}). This dephosphorylation rate decreased fivefold after treatment with NADA (k ~ 0.04 s^{-1}, Figure 4A). Similar results were obtained when 1 mM ADP replaced EGTA, showing that interaction of ADP with the NADA-treated enzyme was decreased (Figure 4B). Analysis of the data using monoexponential decay function yielded a rate constant of 0.821 ± 0.11 s^{-1} for the control enzyme and and 0.229 ± 0.02 s^{-1} for the NADA-treated enzyme.

Cleavage with PrtK

Following incubation of SERCA in the E_1 conformation with PrtK, a cleavage between Thr^{242} and Glu^{243} occurs, producing a C-terminal p83C fragment and an N-terminal p28N fragment (Møller *et al.*, 2002). An additional cleavage at Leu^{119}-Lys^{120} is observed in the E_2 conformation, producing p95C and p14N fragments (Lenoir *et al.*, 2004). We have used PrtK cleavage as a tool to confirm that NADA directly interacted with SERCA and modified its conformation. Hence, control and NADA-treated SR vesicles were phosphorylated from either ATP or P_i, followed by 30 min incubation with PrtK before gel electrophoresis. Phosphorylation was performed at either acidic or neutral pH. At pH 6.2 (Figure 5, left panel), NADA increased accumulation of the p83C fragment, both for enzyme phosphorylated from ATP and P_i. The effect was more pronounced in the ATP phosphorylated enzyme (see

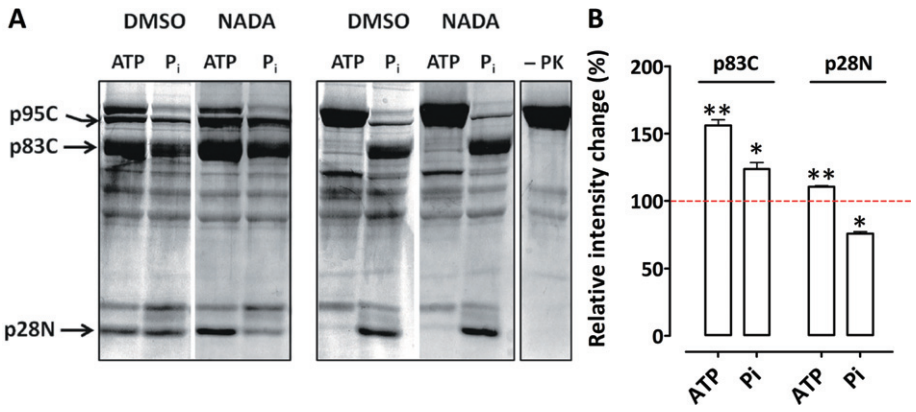

Figure 5

Cleavage with PrtK. (A) SDS-PAGE after cleavage with PrtK. Phosphorylation from ATP was performed as described in Methods. The pH was either pH 6.2 (left panel) or 7.0 (right panel), A representative trace from of five independent experiments is shown. (B) The effect of NADA on the accumulation of the proteolytic fragments p83C and p28N at pH 6.2, expressed as percentage of intensity change induced by NADA compared with cleavage in the presence of DMSO (control), indicated by the dashed line at 100%. Data are mean ± SEM of five measurements. *$P < 0.05$, **$P < 0.01$, significantly different from DMSO controls; two-way ANOVA.

legend to Figure 5). The level of the p95C fragment also increased following NADA treatment. Thus, the level of the p83C fragment increased by 50.2 ± 5.9% in enzyme phosphorylated from ATP and 20.7 ± 3.7% in enzyme phosphorylated from inorganic phosphate. On the other hand, the level of the p28N fragment increased by 10.1 ± 1.1% in enzyme phosphorylated from ATP and decreased by 25.1 ± 3.2% in enzyme phosphorylated from inorganic phosphate (Figure 5B). The decrease in the level of the p28N fragment occurs concurrently with an increase in the level of the p83C and p95C fragments at pH 7 (Figure 5, right panel), NADA had no detectable effect on accumulation of the p83C fragment in enzyme phopshorylated from P_i. However, enzyme phosphorylated from ATP was protected from cleavage, as previously described (Inesi *et al.*, 2008). NADA seems to increase the protection of enzyme phosphorylated from ATP at neutral pH, an effect opposite to that obtained with capsaicin (Mahmmoud, 2008).

Effects of SERCA uncoupling drugs on cytoplasmic ATP levels

One of the primary aims of our work was to validate the anticipated consequences of SERCA uncoupling by NADA. To this end, we have investigated the effect of NADA on ATP levels in human cultured skeletal muscle cells. As seen in Figure 6A, 100 nM NADA was enough to sustain a drastic decrease in cytoplasmic ATP levels, by ~60% after 4 h of treatment. This effect was not observed in the presence of glucose (Figure 6B) and abolished by pretreatment with 400 nM thapsigargin, either in the absence or the presence of glucose (Figure 6C and D). The maximum concentration of NADA used in another set of experiments was 5 μM, which decreased by ~85% the ATP levels, after 4 h of treatment in the absence of glucose. Treatment with 10 μM capsaicin resulted only in a 30% drop in ATP levels (data not shown). Under all conditions, no decrease in cell number or viability was observed. Unpaired *t*-test revealed that thapsigargin had

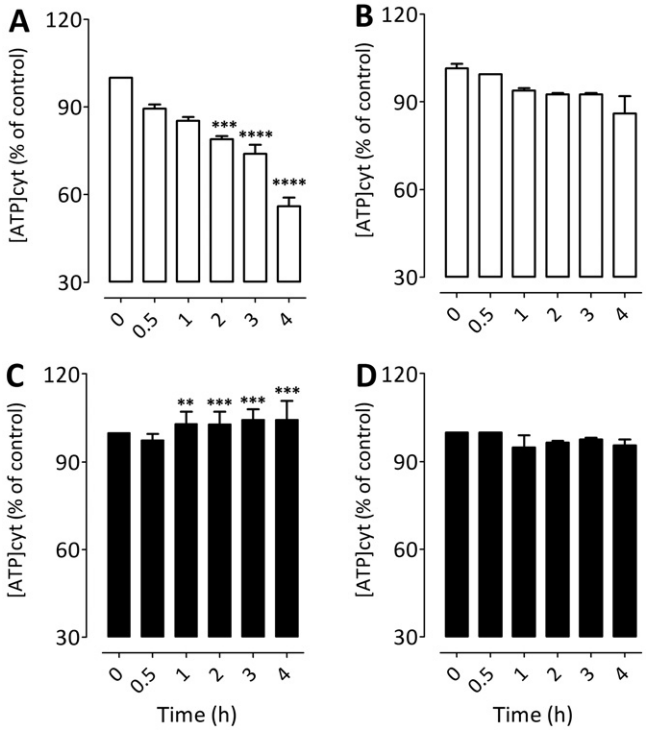

Figure 6

NADA decreased ATP levels in cultured human skeletal muscle cells. Human myotubes were exposed to 0.1 μM NADA supplemented without (panels A and C) or with (panels B and D) 5 mM glucose and without (panel A and B) or with (panels C and D) 400 nM thapsigargin (TG) followed by determination of myocellular ATP content (ATP cyt) after the indicated incubation periods. Myotube isolation and treatment was performed as described in Methods. Data are depicted as a percentage of control, measured at time zero before the addition of ligands. (A) ***$P < 0.001$, ****$P < 0.0001$, significantly different from glucose treated cells; two-way ANOVA. (C) **$P < 0.01$, ***$P < 0.001$, significant effect of thapsigargin; two-way ANOVA.

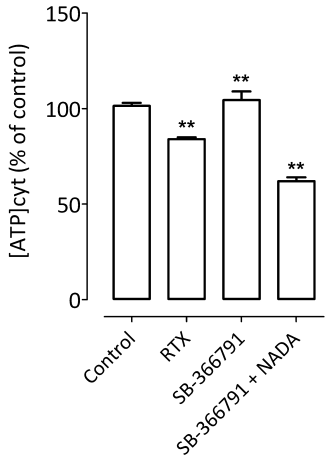

Figure 7

Effect of vanilloid receptor modulators on ATP levels. Human myotubes were exposed to 0.1% DMSO (vehicle control), 5 μM RTX, 10 μM SB-366791, or 10 μM SB-366791 plus 5 μM NADA, as indicated. Following treatment, myotubes were incubated for 4 h, followed by ATP measurement of ATP (ATP cyt), as described in Methods. $^{**}P = 0.001$, significantly different from control; one-way ANOVA.

no statistically significant effect on ATP levels in the presence of glucose ($P > 0.05$), but the effect was significant in its absence ($P < 0.05$). Glucose had a significant effect on ATP levels either in the presence or in the absence of thapsigargin.

NADA affects at least two Ca^{2+} transporting proteins in muscle membranes. Thus, additional control experiments were performed to estimate the effect of NADA on transient receptor potential vanilloid (TRPV) channels, expressed in sarcolemma (Brinkmeier, 2011). Treatment with the vanilloid receptor agonist resiniferatoxin (RTX, 5 μM) resulted in a thapsigargin–sensitive 16% decrease in ATP levels after 4 h (Figure 7), probably representing the component activated by increased passive Ca^{2+} flux and indirect stimulation of the pumping activity of SERCA. The vanilloid receptor antagonist SB-36679 had no effect on ATP levels and addition of NADA decreased ATP levels in cells pretreated with the antagonist, showing that NADA was able to decrease ATP levels, when the TRPV channels were blocked. Experiments using purified SR vesicles established that neither RTX nor SB-36679 modified SERCA-mediated ATP hydrolysis (data not shown). It is also noteworthy to mention that neither RTX or SB-36679 had any effect on the hydrolytic activity of the closely related Na^+/K^+-ATPase, in contrast to the TRPV antagonist capsazepine, which is a potent inhibitor of Na^+/K^+-ATPase.

Discussion and conclusions

NADA synthesis and the mechanism of SERCA modulation

In this study, we provide the first evidence for SERCA uncoupling and consequent ATP depletion mediated by an endogenous compound, NADA, a member of the endocannabinoid family, which has many mechanisms for synthesis, transport and degradation (Wang and Ueda, 2009). NADA is synthesized in brain by conjugation of arachidonic acid with dopamine, a process in which fatty acid amide hydrolase plays an important role (Hu *et al.*, 2009). However, alternative pathways for the synthesis of NADA are possible, for instance, conjugation of arachidonoyl CoA with dopamine or the conversion of arachidonoyl amino acid to NADA. Although fatty acid-binding protein 3 has been shown to act as intracellular carrier for anandamide (Kaczocha *et al.*, 2008), the precise mechanism whereby these molecules are transported across the different cellular compartments is unclear.

Uncoupling of SERCA was inferred from the fact that NADA had no effect on SERCA treated with 20 mM of the uncoupling inhibitor fluoride (Figure 1B). Uncoupling of SERCA implies that energy from ATP hydrolysis dissipates as heat rather than being used to actively transport Ca^{2+} to the SR lumen. Indeed, our measurements with NADA are in good agreement with a previously published model for the uncoupling of SERCA reconstituted into liposomes (Yu and Inesi, 1995). In this model, low stoichiometric efficiency of Ca^{2+} transport (which inevitably leads to increased thermogenesis) was postulated in the absence of passive Ca^{2+} leak under conditions of high Ca^{2+} concentration in the liposome lumen. The existence of an alternative pathway for dephosphorylation that operates at a lower rate than that of the coupled pathway and is associated with Ca^{2+} release to the cytoplasm, was therefore postulated. Similarly, we observed no activation by NADA in the absence of a Ca^{2+} gradient (Figure 2B). NADA decreased the Ca^{2+} affinity of the luminal sites (Figure 3B) and significantly decreased the dephosphorylation rate upon removal of Ca^{2+} (or addition of ADP) to the phosphorylation medium (Figure 4). Because Ca^{2+} occlusion is indispensable for energy utilization, Ca^{2+} occlusion followed by ADP dissociation and Ca^{2+} release to the cytoplasm is crucial for uncoupling to proceed. Mechanistically, this may explain why the effect of NADA was more prominent at lower extra-vesicular Ca^{2+} concentrations (Figure 2A), a condition at which deocclusion of Ca^{2+} back to the cytoplasm is not hindered.

Two related compounds, that have similar structures exerted little or no effect on the hydrolytic activity of SERCA, compared with NADA (Figure 1A), suggesting the requirement of a long chain polyunsaturated fatty acid chain for optimum interaction with the pump. We have recently documented the importance of the position of unsaturation in C18 fatty acids in sustaining important regulatory interactions with Na,K-ATPase (Mahmmoud and Christensen, 2011). Hence, small variations in a group of structurally related molecules can have significant functional differences. It would be valuable to systematically investigate the effect of anandamide and other dopamine amides on vanilloid- and cannabinoid receptors as well as the SERCA pump, as this may provide important pharmacological information in terms of potency and specificity of these molecules against these targets (see below).

NADA modifies the conformational equilibrium of SERCA

As indicated from the inhibition of E_2P formation, the decrease in luminal Ca^{2+} interaction (Figure 3B), and the

effect on cleavage with PrtK (Figure 5) induced by NADA, it is clear that NADA stabilizes an E_1 like form of SERCA. However, the NADA-induced accumulation of the p95C at acidic pH (Figure 5, left panel) indicates that the loop containing Leu[119] is exposed, suggesting a shift to a conformation in which the M_2 domain is away from the M3-M4 domains. Based on earlier data on the role of the A-domain M_2 link in dephosphorylation (Lenoir *et al.*, 2004) and the role of A domain M_1 link in Ca^{2+} release and the $E_1P \rightarrow E_2P$ transition (Daiho *et al.*, 2007), we believe that NADA disrupts the regular communication between the A and P domains such that following Ca^{2+} occlusion and phosphoryl transfer, both the $E_1P \rightarrow E_2P$ transition and ADP interaction is impaired. The latter is indicated from the decreased dephosphorylation rate following quenching with ADP of the NADA-treated enzyme (Figure 4B). NADA was found to protect the p83C complex from cleavage at acidic pH (Figure 5). This is in contrast to capsaicin, which destabilized the complex (Mahmmoud, 2008). Indeed, the protection by NADA of the p83C also implies a modified interaction between the N and P domains.

SERCA uncouplers as novel ATP-depleting agents

An adequate supply of metabolic substrates must be provided to cells to generate ATP, which is obtained by oxidative phosphorylation of pyruvate in mitochondria through the citric acid cycle. In the absence of glucose, oxidative phosphorylation can proceed through acetyl CoA obtained from fatty acids or amino acids. In tissues that have fluctuating energy demands such as skeletal muscle, several systems ensure the prevention of sudden falls in ATP levels under high-intensity muscular activity, and hence ATP levels has to be kept within a narrow range. For instance, the creatine phosphate/kinase system ensures efficient ATP regeneration, such that creatine phosphate levels have to decrease by 90% before normal ATP levels decrease by only 10%. However, in the presence of macrolides that directly inhibit ATP synthesis, ATP levels fall significantly. We now show that increased uncoupled activity of ATP hydrolysing housekeeping enzymes such as SERCA also influenced steady state ATP levels in the absence of compensatory mechanisms that can restore ATP synthesis (Figure 6).

Previous reports have recognized ATP levels as a major determinant of the mechanism of cell death (Eguchi *et al.*, 1997). In addition, the combination of ATP depletion and cancer chemotherapy has been shown to significantly enhance treatment (Martin and Koutcher, 2001). The post mitochondrial strategy proposed here provides a significantly different alternative to the conventional inhibition of proton fluxes in mitochondria. The most widely used ATP-depleting agent, oligomycin, is highly toxic and has low specificity. Indeed, oligomycin injection to rats, although reported to decrease O_2 consumption by 50%, did not affect the level of glucose, pyruvate or lipid metabolites (Kramar *et al.*, 1984). The potential use of capsaicin in cancer treatment may also be related to its hyperthermic effect (Kobayashi *et al.*, 1998), which is not expected to be sustained by macrolides.

Importance of SERCA function in metabolism and metabolic disease control

Recent studies have shown that SERCA is an important control point for the regulation of energy balance in fast- and slow-twitch skeletal muscle in mouse, accounting for 50% of the basic metabolic rate in these cells (Norris *et al.*, 2010). Indeed, decreased SERCA activity in insulin-resistant rats (Wold *et al.*, 2005) as well as restoration of glucose tolerance and euglycemia, induced by overexpression of SERCA 2b in the liver of obese mice (Park *et al.*, 2010) highlights the importance of SERCA in the regulation of endoplasmic reticulum stress and energy balance. We propose that SERCA uncoupling occurring under conditions of low cytoplasmic Ca^{2+} concentration may represent an important mechanism for energy interconversion in resting muscle.

Endocannabinoids have functional effects on several Ca^{2+} handling proteins. For instance, NADA has been shown to inhibit human T-type Ca^{2+} channels expressed in HEK 293 cells (Ross *et al.*, 2009). Hence, auxiliary effects of NADA on Ca^{2+} channels cannot be ruled out. In fact, molecular biology studies on cardiac myocytes have described a highly organized transcriptional cross talk and remodelling of Ca^{2+} signalling following reduction of SERCA 2 expression (Seth *et al.*, 2004). Clearly, some of the effects of endocannabinoids are likely to be mediated through their effects on passive Ca^{2+} transport (TRPV channels). Nonetheless, our data indicate that SERCA uncoupling mediated by these endogenous molecules accounts for at least a major part, as shown by the effect of the specific inhibitor thapsigargin on ATP levels. We have found that arachidonylethanolamide, another endocannabinoid member, also stimulates uncoupled SERCA activity (Y.A. Mahmmoud, unpubl. obs.), suggesting that several members of this family can play a similar role. Together with the fact that TPRV modulators exert differential effects on SERCA, it is likely that endocannabinoid members will have differential effects on several Ca^{2+} handling proteins. Biophysical studies on the effect of several endocannabinoids on reconstituted SERCA are in progress to understand the effect of these molecules on pre steady state events in the Ca^{2+}-ATPase cycle.

Acknowledgements

The authors wish to thank Professor J Møller for the preparation of SR vesicles and for stimulating discussions, Anne Lillevang, Irene Lynfort, and Karin Dyrgaard for excellent technical assistance. Kurt Højlund and Klaus Levin are thanked for muscle biopsies. This work is supported by the Novo Nordic Foundation (Grant A11272 to YAM).

Conflict of interest

The authors declare no conflict of interest.

References

Alexander SPH, Mathie A, Peters JA (2011). Guide to receptors and channels (GRAC), 5th edn. Br J Pharmacol 164 (Suppl. 1): S1–324.

Andersen JP (1995). Dissection of the functional domains of the sarcoplasmic reticulum Ca(2+)-ATPase by site-directed mutagenesis. Biosci Rep 15: 243–261.

Arruda AP, Ketzer LA, Nigro M, Galina A, Carvalho DP, de Meis L (2008). Cold tolerance in hypothyroid rabbits: role of skeletal muscle mitochondria and sarcoplasmic reticulum Ca-ATPase isoform 1 in heat production. Endocrinology 149: 6262–6271.

Balverg MGJ, Verhoeckx KCM, Witkamp RF (2009). Development and validation of a quantitative method for the determination of 12 endocannabinoids and related compounds in human plasma using liquid chromatography-tandem mass spectrometry. J Chromatogr B Analyt Technol Biomed Life Sci 877: 1583–1590.

Barata H, de Meis L (2002). Uncoupled ATP hydrolysis and thermogenic activity of the sarcoplasmic reticulum Ca^{2+}-ATPase: coupling effects of dimethyl sulfoxide and low temperature. J Biol Chem 277: 16868–16872.

Brinkmeier H (2011). TRP channels in skeletal muscle: gene expression, function and implications for disease. Adv Exp Med Biol 704: 749–758.

Daiho T, Yamasaki K, Danko S, Suzuki H (2007). Critical role of Glu^{40}-Ser^{48} loop linking Actuator domain and first transmembrane helix of Ca^{2+}-ATPase in Ca^{2+} deocclusion and release from ADP-insensitive phosphoenzyme. J Biol Chem 282: 34429–34447.

Eguchi Y, Shimizu S, Tsujimoto Y (1997). Intracellular ATP levels determine cell death fate by apoptosis or necrosis. Cancer Res 57: 1835–1840.

Gaster M (2007). Insulin resistance and the mitochondrial link. Lessons from cultured human myotubes. Biochim Biophys Acta 1772: 755–765.

Gaster M, Beck-Nielsen H, Schroder HD (2001a). Proliferation conditions for human satellite cells. The fractional content of satellite cells. APMIS 109: 726–734.

Gaster M, Kristensen SR, Beck-Nielsen H, Schroder HD (2001b). A cellular model system of differentiated human myotubes. APMIS 109: 735–744.

Hu SSJ, Bradshaw HB, Benton VM, Chen JSC, Huang SM, Minassi A *et al.* (2009). The biosynthesis of N-arachidonoyl dopamine, a putative endocannabinoid, via conjugation of arachidonic acid with dopamine. Prostaglandins Leukot Essent Fatty Acids 81: 291–301.

Huang SM, Bisogno T, Trevisani M, Al-Hayani A, De Petrocellis L, Fezza F *et al.* (2002). An endogenous capsaicin-like substance with high potency at recombinant and native vanilloid VR1 receptors. Proc Natl Acad Sci U S A 99: 8400–8405.

Inesi G, Lewis D, Toyoshima C, Hirata A, de Meis L (2008). Conformational fluctuations of the Ca^{2+}-ATPase in the native membrane environment. Effects of pH, temperature, catalytic substrates, and thapsigargin. J Biol Chem 283: 1189–1196.

Kaczocha M, Glaser ST, Deutsch DG (2008). Identification of intracellular carriers for the endocannabinoid anandamide. Proc Natl Acad Sci U S A 106: 6375–6380.

Klodos I, Esmann M, Post RL (2002). Large-scale preparation of sodium-potassium ATPase from kidney outer medulla. Kidney Int 62: 2097–2100.

Kobayashi A, Osaka T, Namba Y, Inoue S, Lee TH, Kimura S (1998). Capsaicin activates heat loss and heat production simultaneously and independently in rats. Am J Physiol 275: R92–R98.

Kramar R, Hohenegger M, Srour AN, Khanakah G (1984). Oliomycin toxicity in intact rats. Agents Actions 15: 660–663.

Kühlbrandt W (2004). Biology, structure and mechanism of P-type ATPases. Nat Rev Mol Cell Biol 5: 282–295.

Lenoir G, Picard M, Gauron C, Montigny C, Maréchal PL, Falson P *et al.* (2004). Functional properties of sarcoplasmic reticulum Ca-ATPase after proteolytic cleavage at Leu119-Lys120, close to the A-domain. J Biol Chem 279: 9156–9166.

MacLennan DH, Rice WJ, Green NM (1997). The mechanism of Ca^{2+} transport by sarco(endo)plasmic reticulum Ca^{2+}-ATPases. J Biol Chem 272: 28815–28818.

Mahmmoud YA (2008). Capsaicin stimulates uncoupled ATP hydrolysis by sarcoplasmic reticulum Ca^{2+}-ATPase. J Biol Chem 283: 21418–21426.

Mahmmoud YA, Christensen SB (2011). Oleic and linoleic acids are active principles in *Nigella sativa* and stabilize an E2P conformation of the Na,K-ATPase. Fatty acids differentially regulate cardiac glycoside interaction with the pump. Biochim Biophys Acta 1808: 2413–2420.

Martin DS, Koutcher A (2001). A concomitant ATP-depleting strategy markedly enhances anticancer agent activity. Apoptosis 6: 125–131.

McCarthy TV, Quane KA, Lynch PJ (2000). Ryanodine receptor mutations in malignant hyperthermia and central core disease. Hum Mutat 15: 410–417.

McGrath J, Drummond G, McLachlan E, Kilkenny C, Wainwright C (2010). Guidelines for reporting experiments involving animals: the ARRIVE guidelines. Br J Pharmacol 160: 1573–1576.

de Meis L, Hasselbach W (1971). Acetyl phosphate as substrate for Ca^{2+} uptake in skeletal muscle microsomes. Inhibition by alkali ions. J Biol Chem 246: 4759–4763.

de Meis L, Arruda AP, Carvalho DP (2005). Role of sarco/endoplasmic reticulum Ca^{2+}-ATPase in thermogenesis. Biosci Rep 25: 181–190.

Mitidieri F, de Meis L (1999). Ca^{2+} release and heat production by the endoplasmic reticulum Ca^{2+}-ATPase of blood platelets. Effect of the platelet activating factor. J Biol Chem 274: 28344–28350.

Møller JV, Lenoir G, Marchand C, Montigny C, le Maire M, Toyoshima C *et al.* (2002). Calcium transport by sarcoplasmic reticulum Ca-ATPase. Role of the A domain and its C-terminal link with the transmembrane region. J Biol Chem 277: 38647–38659.

Norris SM, Bombardier E, Smith IC, Vign C, Tupling AR (2010). ATP consumption by sarcoplasmic reticulum Ca^{2+} pump accounts for 50% of resting metabolic rate in mouse fast and slow twitch skeletal muscle. Am J Physiol Cell Physiol 298: C521–C529.

Olesen C, Sørensen TLM, Nielsen RC, Møller JV, Nissen P (2004). Dephosphorylation of the calcium pump coupled to counterion occlusion. Science 306: 2251–2255.

Olesen C, Picard M, Winther AM, Gyrup C, Morth JP, Oxvig C *et al.* (2007). The structural basis of calcium transport by the calcium pump. Nature 450: 1036–1042.

Park SW, Zhou Y, Lee J, Lee J, Ozcan U (2010). Sarco(endo)plasmic reticulum Ca-ATPase 2b is a major regulator of endoplasmic reticulum stress and glucose homeostasis in obesity. Proc Natl Acad Sci U S A 107: 19320–19325.

Reis M, Farage M, de Souza AC, de Meis L (2001). Correlation between uncoupled ATP hydrolysis and heat production by sacroplasmic reticulum Ca-ATPase: coupling effect of fluoride. J Biol Chem 276: 42793–42800.

Ross HR, Gilmore AJ, Connor M (2009). Inhibition of human recombinant T-type calcium channels by the endocannabinoid N-arachidonoyl dopamine. Br J Pharmacol 156: 740–750.

Scotter EL, Abood ME, Glass M (2010). The endocannabinoid system as a target for the treatment of neurodegenerative disease. Br J Pharmacol 160: 480–498.

Seth M, Sumbilla C, Mullen SP, Lewis D, Klein MG, Hussain A *et al*. (2004). Sarco(endo)plasmic reticulum Ca^{2+} ATPase (SERCA) gene silencing and remodeling of the Ca^{2+} signaling mechanism in cardiac myocytes. Proc Natl Acad Sci U S A 101: 16683–16688.

Sørensen TL, Møller JV, Nissen P (2004). Phosphoryl transfer and calcium ion occlusion in the calcium pump. Science 304: 1672–1675.

Szallasi A, Blumberg PM (1999). Vanilloid (capsaicin) receptors and mechanisms. Pharmacol Rev 51: 159–212.

Toyoshima C, Nakasako M, Nomura H, Ogawa H (2000). Crystal structure of the calcium pump of sarcoplasmic reticulum at 2.6 Å resolution. Nature 405: 647–655.

Toyoshima C, Nomura H, Tsuda T (2004). Lumenal gating mechanism revealed in calcium pump crystal structures with phosphate analogues. Nature 432: 361–368.

Wang J, Ueda N (2009). Biology of endo cannabinoid synthesis system. Prostaglandins Other Lipid Mediat 89: 112–119.

Wold LE, Dutta K, Mason MM, Ren J, Cala SE, Schwanke ML *et al*. (2005). Impaired SERCA function contributes to cardiomyocyte dysfunction in insulin resistant rats. J Mol Cell Cardiol 39: 297–307.

Yu X, Inesi G (1995). Variable stoichiometric efficiency of Ca^{2+} and Sr^{2+} transport by the sarcoplasmic reticulum ATPase. J Biol Chem 270: 4361–4367.